

Shape Coexistence and the $N = 28$ Shell Closure Far from Stability

F. Sarazin,¹ H. Savajols,¹ W. Mittig,¹ F. Nowacki,² N. A. Orr,³ Z. Ren,¹ P. Roussel-Chomaz,¹ G. Auger,¹ D. Baiborodin,⁴ A. V. Belozyorov,⁵ C. Borcea,⁶ E. Caurier,⁷ Z. Dlouhý,⁴ A. Gillibert,⁸ A. S. Lalleman,¹ M. Lewitowicz,¹ S. M. Lukyanov,⁵ F. de Oliveira,¹ Y. E. Penionzhkevich,⁵ D. Ridikas,¹ H. Sakurai,⁹ O. Tarasov,⁵ and A. de Vismes¹

¹GANIL, BP 5027, F-14076 Caen Cedex 05, France

²Laboratoire de Physique Théorique, F-67084 Strasbourg Cedex, France

³LPC, ISMRA et Université de Caen, F-14050 Caen Cedex, France

⁴Nuclear Physics Institute, ASCR, 250 68 Řež, Czech Republic

⁵FLNR, JINR, Dubna, P.O. Box 79, 101 000 Moscow, Russia

⁶IAP, P.O. Box MG-6, 76900 Bucharest-Magurele, Romania

⁷IRES, Université Louis Pasteur, BP 28, F-67037 Strasbourg Cedex 2, France

⁸CEA/DSM/DAPNIA/SPhN, CEN Saclay, F-91191 Gif-sur-Yvette, France

⁹RIKEN, Wako, Saitama 351-01, Japan

(Received 1 December 1999)

The masses of 31 neutron-rich nuclei in the range $A = 29-47$ have been measured. The precision of 19 masses has been significantly improved and 12 masses were measured for the first time. The neutron-rich Cl, S, and P isotopes are seen to exhibit a change in shell structure around $N = 28$. Comparison with shell model and relativistic mean field calculations demonstrate that the observed effects arise from deformed prolate ground state configurations associated with shape coexistence. Evidence for shape coexistence is provided by the observation of an isomer in ^{43}S .

PACS numbers: 21.10.Dr, 21.60.-n, 27.30.+t, 27.40.+z

The stability of nuclei arises from a delicate balance between nuclear, electromagnetic, and weak forces in the nuclear medium. The challenge of a precise modeling of the underlying laws motivates an intense direct investigation of nuclei far from stability that was made possible by the availability of secondary radioactive beams of steadily increasing intensity. In particular, the evolution of shell closures far from stability is a subject of much actual debate [1,2]. Deformations, shape coexistence, or variations in the spin-orbit strength as a function of the neutron to proton ratio could provoke the modification of magic numbers. Such behavior has consequences in other domains, as seen, for example, in nucleosynthesis, where a quenching of shell effects, and consequently of spin-orbit splitting, can provide for a better agreement between model calculations and observed abundances [3]. A breaking of magicity has already been observed at the $N = 20$ shell closure where an island of inversion in shell ordering has been shown to exist [4-6]. More recently, the determination of the lifetime [7] and of the deformation of ^{44}S [8] has indicated the existence of a similar effect at $N = 28$. Interestingly, this is the first shell closure that arises from the spin-orbit splitting, which is responsible for the $1f_{7/2}-2p_{3/2}$ shell gap.

Experimentally, nuclear binding energies are very sensitive to the existence of shells and may provide clear signatures of shell closures [9]. It was in this spirit that a mass measurement experiment using a direct time of flight technique was undertaken to investigate the $N = 20$ and 28 shell closures for nuclei from Ne ($Z = 10$) to Ar ($Z = 18$). The nuclei of interest were produced by the fragmentation of a 60A MeV ^{48}Ca beam on a Ta target located in the

SISSI device. In order to combine the production of nuclei of interest with a broad range of reference masses, the production target, which rotated at ~ 2000 turns/min, was composed of sectors of different thicknesses of 550 (89%), 450 (10%), and 250 mg/cm² (1%). The mass is deduced from the relation $B\rho = \gamma m_0 v/q$ where $B\rho$ is the magnetic rigidity of a particle of a rest mass m_0 , charge q , and velocity v , and γ is the Lorentz factor. This technique has already been used at Ganil to measure the masses of a large number of neutron-rich nuclei [4,10]. The 82 m long flight path between a start detector located near the production target and a stop detector at the final focal plane of the high resolution spectrometer SPEG facilitated the time-of-flight measurement. The magnetic rigidity was measured in the dispersive section of the SPEG spectrometer using a position sensitive detector [11]. Unambiguous particle identification was provided by a four-element silicon detector telescope. A mass resolution corresponding typically to ± 3 MeV of the mass excess was obtained.

Depending on the statistics, a final precision in the mass excess ranging from 100 keV for thousands of events to 1 MeV for tens of events was obtained. The present measurements included the detection of delayed γ rays from isomers by a 4π NaI array surrounding the detector telescope. Of the newly measured nuclei, only ^{43}S exhibited a small ($\sim 1\%$) isomeric contamination, which was too weak to influence significantly the derived mass. As noted above, a large number of well known nuclei transmitted in a single setting provided a calibration from which the new masses were deduced.

A crucial problem in direct mass measurements is the choice of reference masses and the estimation of the

systematic errors. We used as references only masses where three or more independent and coherent mass determinations were available. Further details of the analysis can be found in Ref. [12]. The present results and recently published mass determinations [13] allowed us to analyze unpublished data [14] from Ref. [4], where a lack of reference masses did not allow masses to be extracted for nuclei heavier than $A = 37$. The results of the present and the reanalyzed data are given in Table I. Listed are all nuclei in the region covered by our measurements where less than three independent measurements were available. As can be seen, the precision for 19 masses was considerably improved, often by a factor of 2 or more. Twelve masses were measured for the first time, eight of them with a precision of better than 1 MeV. The errors cited contain the statistical error and a systematic error, based on the extrapolation procedures. No statistically significant discrepancies with previous measurements and between the two new sets of results were observed. In the last column of Table I the weighted mean values of the

different mass determinations are given and these values are used in the following discussion.

The separation energy of the two last neutrons corresponding to a derivative of the mass surface, S_{2n} , derived from the current (Table I) and previous measurements [13] are displayed in Fig. 1. The Ca isotopes show the behavior typical of the filling of shells, with the two shell closures at $N = 20$ and 28 being evidenced by the corresponding sharp decrease of the S_{2n} , and a slowly decreasing S_{2n} as the $1f_{7/2}$ shell is filled. The K and Ar isotopes show a similar behavior. The Cl, S, and P isotopes, however, exhibit a pronounced change of slope around $N = 26$.

A more direct way to see shell effects on nuclear masses is to subtract the “macroscopic” contribution. Here we have used the finite range liquid drop model of Ref. [15]. The difference—the microscopic or the shell correction energy—is plotted in Fig. 2, together with predictions of the shell model [6,16]. As in Fig. 1, the qualitatively different behavior of the S and P isotopes as compared to the Ca isotopes is clearly evident. The Ca isotopes show

TABLE I. Experimental mass excesses (\pm uncertainties in keV). The first column is from the present experiment, the second column is from reanalyzed data [14], the third column is the weighted mean value of the first and second columns, the fourth column is from the compilation of Audi *et al.* [13], and the last column is the weighted mean of the third and fourth columns.

	Present	Reanalysis [14]	Mean(Pres. + Rean.)	Ref. [13]	Weighted Mean
²⁹ Ne	18 070 (380)			18 020 (300)	18 050 (240)
³⁰ Ne	23 900 (790)			22 240 (820)	23 100 (570)
³² Na	19 540 (470)			18 300 (480)	19 020 (350)
³³ Na	24 560 (1080)			25 510 (1490)	24 880 (880)
³⁴ Mg	9220 (330)			8450 (260)	8760 (210)
³⁵ Mg	17 540 (1000)	17 400 (1600) [4]	17 500 (850)		17 500 (850)
³⁶ Mg	23 220 (1500)				23 220 (1500)
³⁶ Al	5720 (290)			5920 (270)	5830 (200)
³⁷ Al	10 150 (420)			9600 (540)	9940 (330)
³⁸ Al	16 750 (860)	14 200 (1400)	16 050 (730)		16 050 (730)
³⁹ Al	21 400 (1470)				21 400 (1470)
³⁸ Si	-3820 (300)	-4200 (170)	-4110 (150)	-3740 (270)	-4020 (130)
³⁹ Si	2060 (460)	1770 (500)	1930 (340)		1930 (340)
⁴⁰ Si	5760 (690)	4930 (940)	5470 (560)		5470 (560)
⁴¹ Si	13 560 (1840)				13 560 (1840)
³⁸ P	-15 010 (290)	-14 820 (130)	-14 850 (120)	-14 470 (140)	-14 690 (90)
³⁹ P	-12 920 (260)	-12 940 (130)	-12 940 (120)	-12 650 (150)	-12 830 (90)
⁴⁰ P	-7640 (300)	-8200 (190)	-8040 (160)	-8340 (200)	-8160 (130)
⁴¹ P	-4930 (390)	-5520 (280)	-5320 (230)	-4840 (470)	-5230 (210)
⁴² P	1440 (590)	240 (690)	930 (450)		930 (450)
⁴³ P	5770 (970)	3930 (1510)	5230 (820)		5230 (820)
⁴⁰ S	-23 200 (320)	-22 770 (180)	-22 870 (160)	-22 850 (230)	-22 870 (130)
⁴¹ S	-19 030 (310)	-19 100 (140)	-19 090 (130)	-18 600 (210)	-18 970 (110)
⁴² S	-18 060 (330)	-17 640 (140)	-17 700 (130)	-17 240 (330)	-17 650 (120)
⁴³ S	-12 020 (430)	-11 930 (230)	-11 950 (200)	-12 480 (840)	-11 980 (200)
⁴⁴ S	-8350 (580)	-9790 (540)	-9120 (400)		-9120 (400)
⁴⁵ S	-3100 (2680)	-3360 (2290)	-3250 (1740)		-3250 (1740)
⁴³ Cl	-24 230 (310)	-24 300 (280)	-24 270 (210)	-24 030 (160)	-24 120 (130)
⁴⁴ Cl	-20 630 (340)	-20 210 (120)	-20 260 (110)	-19 990 (220)	-20 200 (100)
⁴⁵ Cl	-18 490 (430)	-18 340 (130)	-18 350 (120)	-18 910 (650)	-18 370 (120)
⁴⁶ Cl	-13 920 (1610)	-14 900 (800)	-14 710 (720)		-14 710 (720)
⁴⁷ Ar	-24 750 (1270)			-25 910 (100)	-25 900 (100)

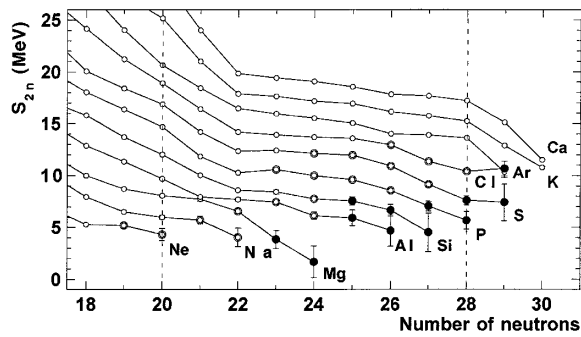


FIG. 1. Experimental S_{2n} values in the region of the $N = 20$ and 28 shell closures. The circles correspond to values from Ref. [13], the bold circles to values for which the precision was improved, and the filled circles to masses measured for the first time (Table I).

pronounced shell correction minimas around $N = 20$ and 28. The S and P isotopes do not exhibit such effects at $N = 28$, and instead show a discontinuity in the slope at $N = 26$. The observed trends are well reproduced by large scale shell model (SM) calculations undertaken within the sd - fp model space [6]. We obtained a similar agreement in relativistic mean field (RMF) calculations [12,17].

Minimization of the potential energy in the RMF model was performed with constrained quadrupole deformations. The results of such calculations including even odd nuclei is shown in Fig. 3 for the S isotopes. Interestingly, beginning at $N = 23$, two local minima were found, cor-

responding to prolate and oblate configurations. Furthermore, for $N \geq 27$, the difference in binding energies for the two solutions suddenly decreases, thus suggesting the coexistence of nearly degenerate different shapes. Similar conclusions have been reached for even-even nuclei in this region by [1,18–20]. Up to now, however, no experimental evidence for shape coexistence in this region has been available, in spite of much theoretical effort [21].

Shape coexistence is often associated with isomerism (see, for example, Ref. [22]). We observed, as described above, an isomeric state in ^{43}S . In a subsequent experiment employing a much shorter flight path (~ 43 m) [23], the energy of the γ rays and the half-life were measured by delayed coincidences between two Ge detectors and a Si telescope. A single transition with $E_\gamma = 319$ keV and a lifetime of 478(48) ns was observed (Fig. 4). The isomeric transition must thus lead directly to the ground state or a very low-lying state ($E_x \leq 50$ keV). For $E1$ and $M1$ transitions such a long lifetime would correspond to a very large hindrance factor and only an $E2$ transition is compatible with the observation. In this case a $B(E2)$ of $0.517(0.052)e^2 \text{ fm}^4$, or 0.04 Weisskopf units, is deduced. Such an isomeric state is predicted by SM calculations similar to those of Ref. [6] as a shape isomer whereby the weak strength of the transition arises from the two very different wave functions involved.

A recent measurement of the Coulomb excitation of ^{43}S revealed a new level at 940 keV with a $B(E2)$ of $175(69)e^2 \text{ fm}^4$ [24]. The SM predictions are compared to experiment in Fig. 4. As can be seen, both the transition strengths and the energies of the levels are well reproduced. In the case of a closed $f_{7/2}$ shell, the ground state of ^{43}S would correspond to a $7/2^-$ neutron hole. The SM, however, predicts an inversion of the $7/2^-$ and the $3/2^-$ levels with the former being the isomeric state. Analysis of the SM wave functions reveals that 48% of the $3/2^-$ ground state corresponds to coupling of a neutron to a deformed core of protons in a 2^+ state. A similar conclusion was reached by [25]. RMF calculations (see Fig. 3) predict

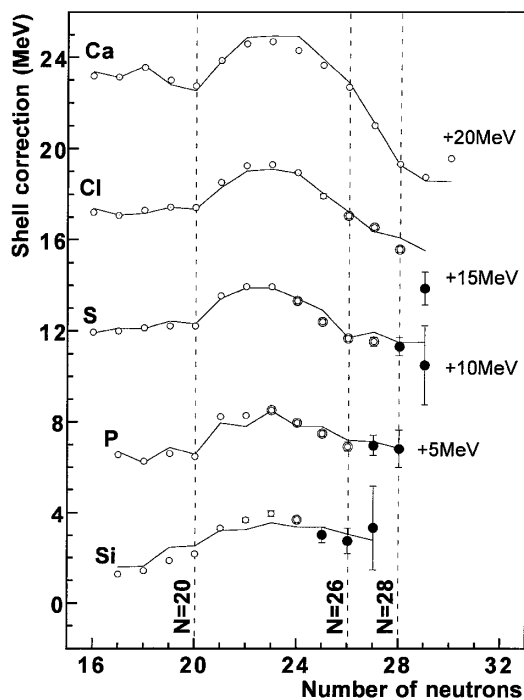


FIG. 2. Shell corrections as defined in the text of the mass of Si, P, S, Cl, and Ca isotopes. The points correspond to experimental values (see caption of Fig. 1 for details), the lines to shell model calculation [6,16].

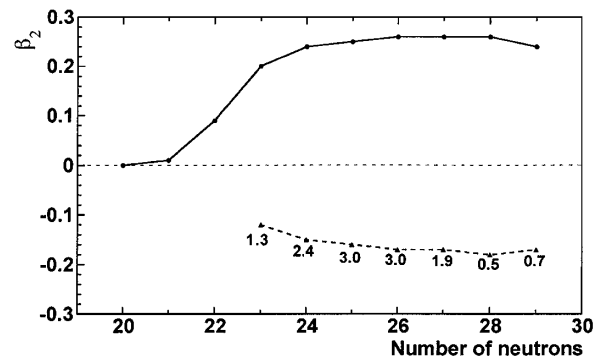


FIG. 3. Quadrupole deformations for S isotopes obtained in the RMF model by maximization of the binding energy. The numbers in the figure are the excitation energy in MeV of the oblate with respect to the prolate configurations.

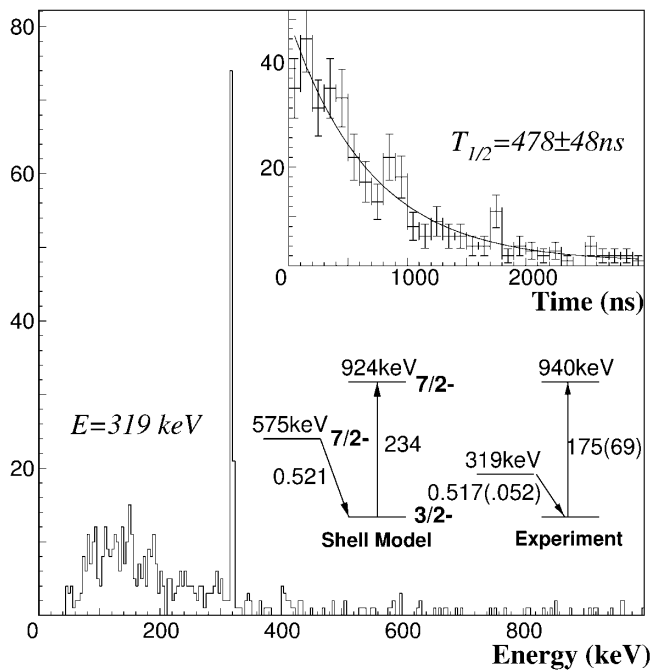


FIG. 4. Experimental spectra for the isomeric state in ^{43}S . The lower inset compares the SM predictions and the experimental values; the numbers besides the transitions are $B(E2)$ values in units of $e^2 \text{fm}^4$.

prolate deformed ground states in this region. In addition, deformation is suggested by the measured $B(E2)$ values [8,24]. The discontinuity observed at $N = 26$ (Fig. 1) can now be understood in a simple Nilsson picture. For a prolate deformation of $\beta_2 \approx 0.2$, a large gap appears between the lowest three orbits and the fourth orbital arising from the $1f_{7/2}$ and higher orbitals. Consequently, a pseudoshell closure due to deformation can be considered to appear at $N = 26$. Oblate deformations would not be compatible with these observations.

As can be seen in Fig. 1, interesting new results have been obtained too, for Ne to Al isotopes. In particular, the steep decrease of the S_{2n} for $^{35,36}\text{Mg}$ suggests that the Mg isotopes may become unbound at a much lower neutron number than the predicted value of $N \geq 28$ [2,26].

In summary, we have measured the masses of 31 neutron-rich nuclei (12 for the first time) in the vicinity of the $N = 20$ and 28 shell closures. The measurements demonstrate that the shell structure for Cl, S, and P isotopes is

modified and a pseudoshell closure arising from deformation appears at $N = 26$. These findings were reproduced by shell model and relativistic mean field calculations. The models predict the appearance of prolate deformations of the ground state in this region and, in particular, the coexistence of different configurations. Evidence for this coexistence was provided by the observation of an isomer in ^{43}S that is well described by shell model calculations. Any future mass measurements beyond $N = 28$ will be of interest as they should provide information on the associated shell gap.

-
- [1] T.R. Werner *et al.*, Phys. Lett. B **335**, 259 (1994); Nucl. Phys. **A597**, 327 (1996).
 - [2] Z. Ren *et al.*, Phys. Lett. B **380**, 241 (1996).
 - [3] B. Pfeiffer *et al.*, Z. Phys. A **357**, 235 (1997).
 - [4] N.A. Orr *et al.*, Phys. Lett. B **258**, 29 (1991).
 - [5] E.K. Warburton *et al.*, Phys. Rev. C **41**, 1147 (1990).
 - [6] J. Retamosa *et al.*, Phys. Rev. C **55**, 1266 (1997).
 - [7] O. Sorlin *et al.*, Phys. Rev. C **47**, 2941 (1993).
 - [8] T. Glasmacher *et al.*, Phys. Lett. B **395**, 163 (1997).
 - [9] W. Mittig, A. Lépine-Scilly, and N. Orr, Annu. Rev. Nucl. Part. Sci. **47**, 27 (1997).
 - [10] A. Gillibert *et al.*, Phys. Lett. B **176**, 317 (1986); **192**, 39 (1987).
 - [11] O.H. Odland *et al.*, Nucl. Instrum. Methods Phys. Res., Sect. A **378**, 149 (1996).
 - [12] F. Sarazin, Thèse, Université de Caen, 1999; Report Ganil-T99 03, 1999.
 - [13] G. Audi *et al.*, Nucl. Phys. **A624**, 1 (1997).
 - [14] N.A. Orr and W. Mittig (unpublished).
 - [15] P. Moller and J.R. Nix, At. Data Nucl. Data Tables **59**, 185 (1995).
 - [16] E. Caurier *et al.*, Phys. Rev. C **58**, 2033 (1998).
 - [17] Z. Ren, RMF code, information on request.
 - [18] G.A. Lalazissis *et al.*, Phys. Rev. C **60**, 014310 (1999).
 - [19] B.V. Carlson and D. Hirata, Report No. RIKEN-AF-NP-303 (to be published).
 - [20] P.G. Reinhard *et al.*, Phys. Rev. C **60**, 014316 (1999).
 - [21] J.L. Woods *et al.*, Nucl. Phys. **A651** 323 (1999), and references therein.
 - [22] F. Becker *et al.*, Eur. Phys. J. A **4**, 103 (1999).
 - [23] A. de Vismes *et al.*, Report No. PE291; thesis in preparation.
 - [24] R.W. Ibbotson *et al.*, Phys. Rev. C **59**, 642 (1999).
 - [25] P.D. Cottle *et al.*, Phys. Rev. C **58**, 3761 (1998).
 - [26] P.E. Haustein, editor, At. Data Nucl. Data Tables **39**, 185 (1988).